



ORIGINAL ARTICLE

Multivariate optimization of differential pulse polarographic–catalytic hydrogen wave technique for the determination of nickel(II) in real samples



S. Kanchi *, M.I. Sabela, P. Singh, K. Bisetty *

Department of Chemistry, Durban University of Technology, P.O. Box 1334, Durban 4000, South Africa

Received 14 May 2013; accepted 31 July 2013

Available online 9 August 2013

KEYWORDS

Differential pulse polarographic–catalytic hydrogen wave (DPP–CHW); Nickel(II); Box–Behnken design; Ammonium piperidine dithiocarbamates (APDC) and Ammonium morpholine dithiocarbamate (AMDC); Cyclic voltammetry; Density Functional Theory (DFT)

Abstract Multivariate optimized experimental conditions were established for the determination of nickel(II) in 92 grape samples after complexation with ammonium piperidine dithiocarbamate (APDC) and ammonium morpholine dithiocarbamate (AMDC). Differential pulse polarographic (DPP) studies of the wave characteristics indicated that it is of the catalytic hydrogen wave (CHW) type sensitive to pH, concentration and scan rates. A single, sharp peak obtained at -1.22 V allowed for the trace determination of nickel(II) in the range of 3.2×10^{-6} to 1.17×10^{-3} M with a linear calibration and a detection limit of 1.8×10^{-6} and 2.7×10^{-6} M for APDC and AMDC respectively. Mechanistic aspects between APDC/AMDC and nickel(II) were confirmed with cyclic voltammetry and supported by theoretical calculations. The DFT calculations of piperidine adduct reveal a smaller HOMO–LUMO energy gap than morpholine adduct, suggesting that piperidine adduct has a greater tendency to act as an electron donor.

© 2013 Production and hosting by Elsevier B.V. on behalf of King Saud University. This is an open access article under the CC BY-NC-ND license (<http://creativecommons.org/licenses/by-nc-nd/3.0/>).

1. Introduction

Nickel is one of many trace metals widely distributed in the environment, being released from both natural sources and anthropogenic activities. Natural sources of atmospheric nickel levels include wind-blown dust, derived from the weathering of rocks and soils, volcanic emissions, forest fires and vegetation. Nickel finds its way into the ambient air as a result of the combustion of coal, diesel oil & fuel oil, the incineration of waste, sewage and miscellaneous sources (Bencko, 1983; Grandjean, 1984; Clarkso, 1988; WHO, 1991; Von Burg, 1997; Spectrum, 1998). Nickel concentrations in ambient air

* Corresponding authors. Tel.: +27 31 3733004/3732311; fax: +27 86 6740243.

E-mail addresses: suvarthank@gmail.com (S. Kanchi), bisettyk@dut.ac.za (K. Bisetty).

Peer review under responsibility of King Saud University.



Production and hosting by Elsevier

vary considerably in the range of 0.01–770 $\mu\text{g L}^{-1}$ depending upon the areas. Drinking water generally contains nickel at concentrations $< 10.0 \mu\text{g L}^{-1}$ (Bencko, 1983; Cott Fordsmand, 1997). Human exposure to highly polluted nickel-environments has the potential to produce a variety of pathological effects. Among them are skin allergies, lung fibrosis, cancer of the respiratory tract and nickel poisoning (Kasprzak et al., 2003).

Experimental design plays a significant role in the enhancement of the quality of analytical data process for method development and validation (Green, 1996; Thomposon et al., 2002). At the same time the validation must be cost effective and internationally acceptable in order to encourage all scientists to make use of it (Thomposon et al., 2002). However, in some cases it was found that the optimized analytical protocols developed with standard samples did not include validation and application of the method. As a consequence of this, the un-validated methods are allowed to assume the aura of validity and authenticity, when, in practice, they may never be completely useful with samples that are typically encountered (Swartz and Krull, 1997). More specifically, experimental design helps the researcher to verify changes in factor values in relation to the observed response by a well-defined mathematical model. Hence, experimental design is considered as a valuable tool for the validation and optimization of variable parameters in the multivariate experimental design systems (Lewis et al., 1999; Montgomery, 1997).

These strategies can be achieved more effectively with the help of a statistical design to monitor the traceability, validation and optimization process in all stages of the experiment (Swartz and Krull, 1997). In particular, during method optimization some performance parameters should be investigated in order to avoid serious problems during the validation step. The performance parameters to evaluate, prior to the validation process include accuracy, precision, robustness, and the evaluation of these parameters are often referred to as the pre-validation stage (Montgomery, 1997; Carlson, 1992; Pieniaszek, 1999). Strategies used for the experimental optimization studies include method precision (repeatability), Taguchi approach (Mathieu et al., 1998), Box–Meyer approach (Box and Meyer, 1986), artificial neural networks (Polaskova et al., 2002) or experimental design methodology (Furlanetto et al., 2003).

Several analytical techniques such as flame atomic absorption spectrometry (Khorrami et al., 2004; Baytak and Rehber Turker, 2006; Dadfarnia et al., 2010; Şahin et al., 2010; Ghaedi et al., 2007), graphite furnace atomic absorption spectrometry (Sun et al., 2006; Dobrowolski and Otto, 2012; Bidabadi et al., 2009), electro-thermal atomic absorption spectrometry (Sadeghi et al., 2011), atomic fluorescence spectrometry (Zeng et al., 2012), spectrophotometry (Amin et al., 2012; Fakhari et al., 2005; Hussain Reddy et al., 2003; Deng et al., 2013; Ramachandraiah et al., 2008; Loka et al., 2008) and inductively coupled plasma optical emission spectrometry (Beiraghi et al., 2012; Silva et al., 2009) have been proposed for the analysis of nickel(II), but most of these require expensive equipment, time consuming sample preparation procedures. However, the electrochemical analysis of trace amounts of nickel(II) requires relatively inexpensive equipment and presents certain difficulties due to their irreversible reduction behaviour (Armstrong et al., 1997; Flora and Nieboer, 1980). Therefore it is needless to say, it has successfully been accom-

plished using a variety of electro-analytical techniques such as stripping & voltammetric analysis (Sancho et al., 2000; Wang et al., 2000; Economou and Fielden, 1998; Colombo and Van der Berg, 1998; Korolczuk, 2000; González et al., 2002) including polarography (Saraswathi et al., 2006).

In this paper, we present a modern eco-friendly method that does not require elaborate clean-up procedures for the extraction of APDC/AMDC-nickel(II) complexes into the organic solvents, thus prohibiting the use of hazardous and environmentally unfriendly chemicals such as chloroform and carbon tetrachloride (Merck and Co, 1983; Hemasundaram, 2006). A literature survey revealed that this study is the first of its kind to apply the Box Behnken experimental design to the differential pulse polarographic catalytic hydrogen wave (DPP-CHW) technique for the determination of nickel(II) using dithiocarbamates (DCs) as ligands in grape samples. Accordingly, we developed a more facile, sensitive, rapid and robust method for the determination of nickel(II) in different grape samples with APDC/AMDC resulting in catalytic hydrogen currents generated at dropping mercury electrode (DME) by differential pulse polarography (DPP). In this regard the experimental design was convenient to evaluate the statistical significance of the variation in current responses due to factor variations and optimization of the related parameters.

Additionally, the reliability of the proposed method with the DPP results on both the piperidine and morpholine adducts with carbon disulphide (CS_2) was validated with theoretical calculations performed at the density functional (DFT) level. The primary aim of these calculations was to compute the HOMO–LUMO energy gaps of these adducts, and to relate them to their electron donating capacities during complexation with the electron deficient metals.

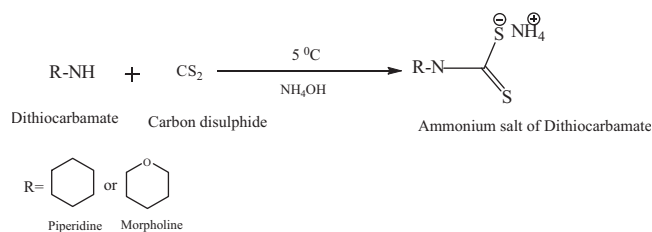
2. Experimental

2.1. Apparatus

A Metrohm model 797 VA Computrace three electrode system (Metrohm Herisau, Switzerland) consists of the hanging mercury dropping electrode (HMDE) as the working electrode for cyclic voltammetric measurements, while the dropping mercury electrode (DME) was used as the working electrode to obtain all the polarographic waves. The reference electrode was Ag/AgCl and platinum wire was used as the counter electrode. All pH measurements were carried out with Crison micro pH model 2000 pH meter. All grape samples were digested with a temperature controllable 100 Teflon PFA vessel microwave digester (CEM MARS-5, CEM Co., USA).

2.2. Chemicals and reagents

All the experiments were performed at 25 °C using freshly prepared solutions. Double distilled mercury was supplied by Metrohm (Durban, South Africa (SA)) and deionized water was generated from an aqua MAX™ – Basic 360 series water purification system from TRILAB SUPPORT (Durban, SA). The dissolved oxygen in the solutions was removed by passing 99.8% pure nitrogen gas (AFROX Durban, SA) for 15 min. Nickel(II) standard solution was prepared by accurately weighing 4.050 g L^{-1} of $\text{NiCl}_2 \cdot 6\text{H}_2\text{O}$ (Merck Laboratory Sup-



Scheme 1 Reaction route for the preparation of ammonium salt of piperidine/morpholine dithiocarbamates.

pliers Pty Ltd, RSA) to get approximately $1.0 \mu\text{g L}^{-1}$ and by adding 3.0 mL of concentrated HNO_3 corresponding to the anions of the salts to suppress the hydrolysis. 1.0 M ammonium chloride was prepared by weighing 53.49 g and dissolving in 1.0 L with deionised water and the pH adjusted with 5% (v/v) ammonium hydroxide and 1% (v/v) hydrochloric acid solutions. Carbon disulphide, piperidine and morpholine were also purchased from Merck Laboratory Suppliers Pty Ltd, SA.

2.2.1. Synthesis of ammonium piperidine/morpholine dithiocarbamates (APDC/AMDC)

Carbon disulphide (80 g) was slowly added to each solution of (85 g) piperidine and morpholine dissolved to 25 mL with distilled water at 5°C under constant stirring, followed by addition of 20% (v/v) ammonium hydroxide for neutralization. The resultant reaction mixture was warmed at room temperature and washed repeatedly with acetone of 99.5% purity. The product was purified by recrystallization in acetone (Hemasundaram, 2006) with melting points ranging from $196\text{--}199^\circ\text{C}$ and $182\text{--}185^\circ\text{C}$ for APDC and AMDC respectively, at 740 mm pressure as shown in Scheme 1.

2.3. DPP-CHW methodology

A measured volume of the $\text{NH}_4\text{Cl-NH}_4\text{OH}$ buffer and ligands (APDC/AMDC) was added to adequate amounts of electroac-

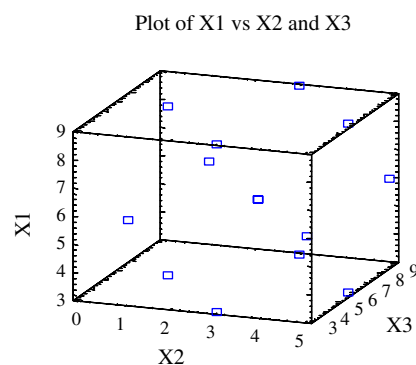


Figure 1 Shows the random distribution of the three factors pH (X1), concentration of DCs (X2) and scan rate (X3).

tive species [nickel(II)]. Dissolved oxygen was removed by bubbling pure nitrogen through the solution in the polarographic cell for 15 min. Polarograms of the solutions were recorded using differential pulse polarography (DPP) at -1.22 V vs Ag/AgCl in ammonium chloride-ammonium hydroxide medium for APDC and AMDC respectively. All cyclic voltammograms were recorded in HMDE mode.

2.4. Preparation of grape samples

A total of 92 grape samples (46 red and 46 white) were collected from local markets and also directly from the farm houses. The grapes were rinsed with 20% (v/v) HNO_3 and stored at 4°C in plastic bags. Six of each type of grape samples were used for recovery studies and the rest (10 red and 10 white from one source) were subdivided into two sets. The first set containing 5 red and 5 white was washed manually for 5 min with deionized water while the other set was analysed without any washing. The investigation was done in epicarp (grape peel), endocarp (grape pulp) with seeds and whole grapes giving a total of 120 samples excluding the spiked samples.

Table 1 Experimental design using APDC (experiment 1) and AMDC (experiment 2).

ID	pH	Conc. of DTC/mM	Scan rate (mV/s)	Experiment 1		Experiment 2	
				APDC		AMDC	
				*Current/ nA	*Potential/V	*Current/nA	*Potential/V
1	3.0	3.0	9.0	1260	-1.54	5.127	-1.38
2	6.0	5.0	9.0	171.9	-1.22	70.66	-1.22
3	3.0	5.0	6.0	641.0	-1.50	62.57	-1.32
4	6.0	5.0	3.0	390.1	-1.22	142.0	-1.22
5	3.0	1.0	6.0	2252	-1.59	71.74	-1.57
6	6.0	3.0	6.0	185.4	-1.22	71.74	-1.22
7	6.0	3.0	6.0	182.5	-1.21	70.16	-1.22
8	3.0	3.0	3.0	1131	-1.54	7456	-1.39
9	9.0	3.0	3.0	173.4	-1.23	75.38	-1.22
10	6.0	3.0	6.0	159.3	-1.22	61.99	-1.22
11	9.0	1.0	6.0	46.07	-1.22	17.86	-1.22
12	9.0	5.0	6.0	145.0	-1.22	58.01	-1.22
13	6.0	1.0	3.0	120.6	-1.22	43.25	-1.22
14	9.0	3.0	9.0	73.63	-1.22	25.60	-1.25
15	6.0	1.0	9.0	67.85	-1.22	28.85	-1.22

* The average current/potential reported for three replicates.

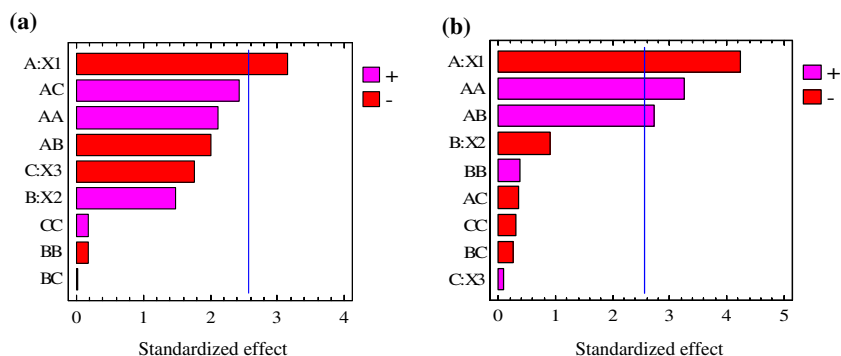


Figure 2 Shows the standardized pareto charts for current response using (a) APDC and (b) AMDC.

Table 2 Estimated effects based on total error and interactions.

Experiment	Source	Sum of squares	Mean square	F-ratio	P-value
1 ^a	pH (X1)	3.35×10^7	1.68×10^7	3.86	0.0672
	Conc. of Ligand (X2)	5.14×10^6	2.57×10^6	0.59	0.5762
	Scan rate (X3)	7.27×10^6	3.64×10^6	0.84	0.4679
2 ^b	pH (X1)	2.94×10^6	2.94×10^6	13.9	0.0034
	Conc. of Ligand (X2)	1.62×10^5	1.62×10^5	0.76	0.4005
	Scan rate (X3)	7.35×10^3	7.35×10^3	0.03	0.8557

^a APDC.

^b AMDC used as complexation ligands.

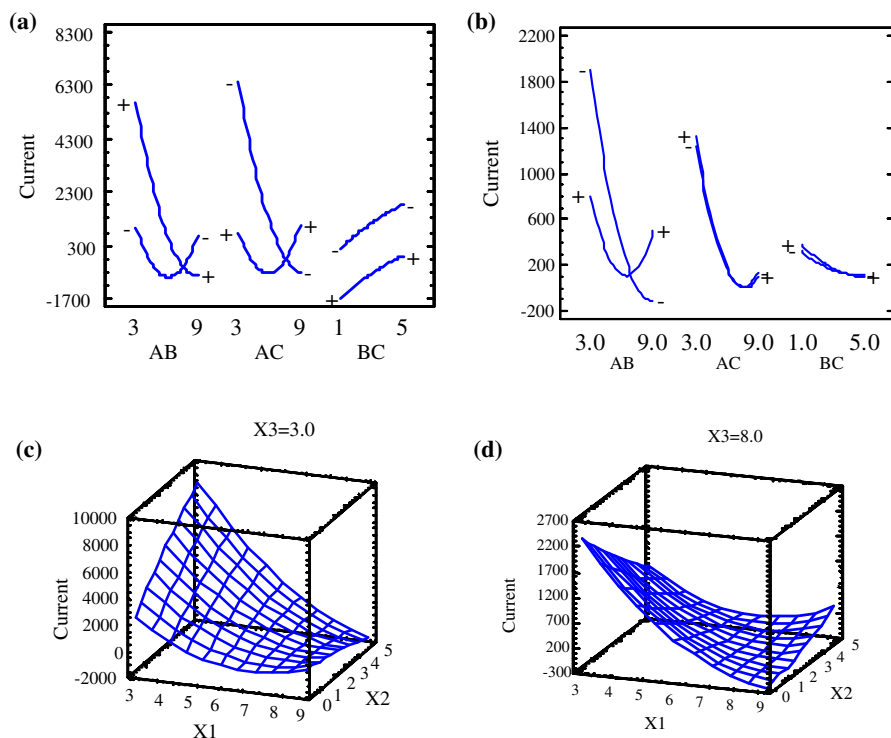


Figure 3 (a) and (b) Interaction plots for current response at different combinations of the three variables. (c) and (d) show the estimated response surfaces for experiment 1 and 2 respectively.

The three sample sets were packed in a decontaminated poly vinyl chloride tube and placed in a micro-wave oven separately at 60 °C for 10 h for epicarp, 12 h for endocarp along

with seeds, and 15 h for the whole grape samples. The dried samples were powdered and transferred into a closed 50 mL Teflon container for digestion process. Approximately 1.0 g

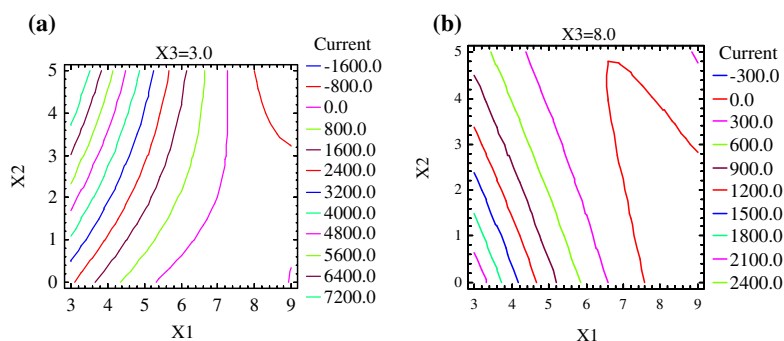


Figure 4 (a) and (b) Show contours of estimated response surface, a clear indication of the relationships between pH (X1) and concentration of DCs (X2) at optimum scan rates (X3).

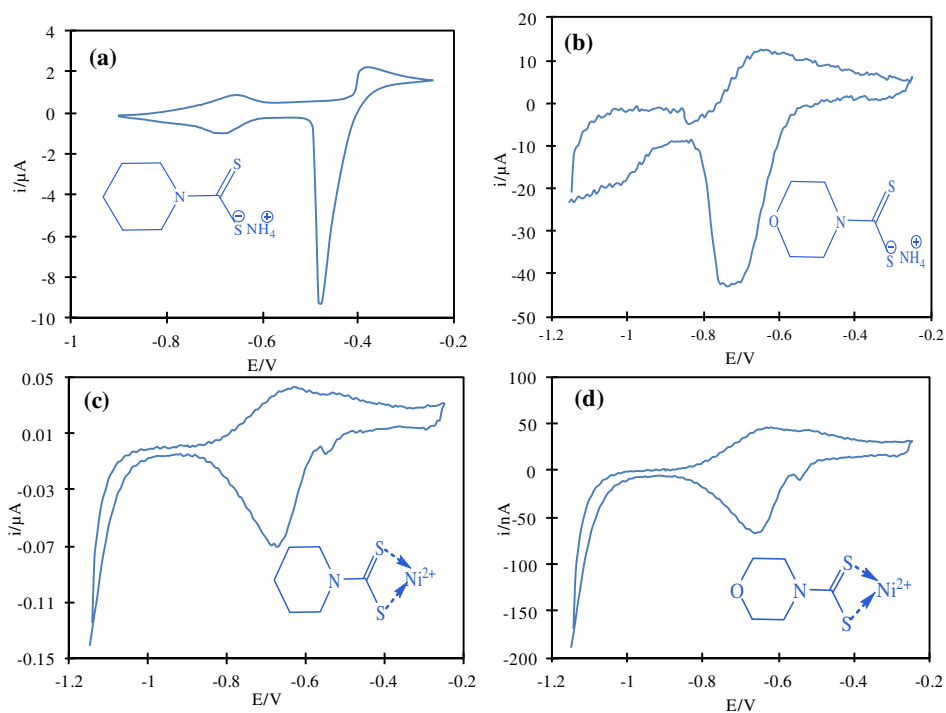


Figure 5 Cyclic voltammograms for (a) 5.0 mM APDC in 0.4 M NH_4Cl at pH 3.0, (b) 1.0 mM AMDC in 0.3 M NH_4Cl at pH 3.0, (c) 5.0 mM APDC + 0.05 ppm nickel(II) in 0.4 M NH_4Cl at pH 3.0, (d) 1.0 mM AMDC + 0.05 ppm nickel(II) in 0.3 M NH_4Cl at pH 3.0.

of powdered sample was accurately weighed and transferred into a closed Teflon container, to which 2.0 mL of HNO_3 , 1.0 mL of HCl and 0.5 mL of H_2O_2 were added. The whole sample system was placed in a micro-wave oven at 90°C for 2 h to complete the digestion process then transferred into a decontaminated poly vinyl chloride tube and diluted with deionized water up to 10 mL and used as a sample for nickel(II) analysis as mentioned above.

2.5. Experimental design

A Box–Behnken design with fifteen runs, three independent variables (pH, scan rate and concentration of ligand) and three replicates at a centre point was used in this study. The experiment was designed such that it was randomized to reduce confounding variables by equalizing the three inde-

pendent variables that have not been accounted for in the experimental design. Table 1 shows the experimental design of the three factors pH, concentration of dithiocarbamates (DCs) and scan rate. The maximum current signals and their respective potentials due to nickel(II) were taken as the response of the designed experiments per DC for the three replicates. Since the two ligands (APDC/AMDC) were used in the study, the design was therefore duplicated with experiment 1 referring to the analysis performed in the presence of APDC, while experiment 2 refers to AMDC. The statistical analysis on the response of the model was performed with an analysis of variance (ANOVA), pareto charts, interaction plots and surface responses. Interestingly, the design enabled us to evaluate the responses with respect to the simultaneous factor variations in all the experimental regions studied and to optimize the experimental conditions for the detection of

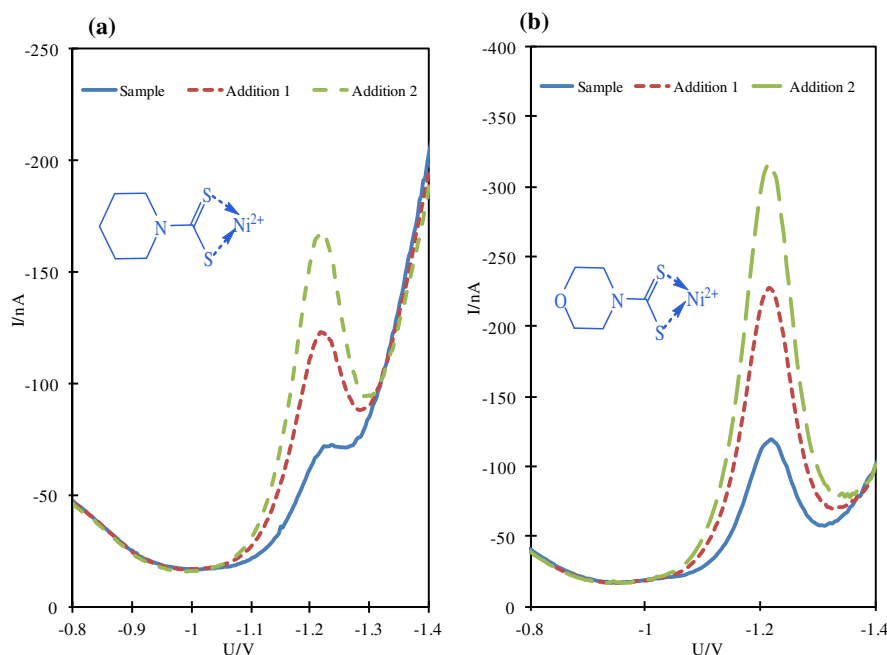


Figure 6 Obtained polarograms in grape samples after optimization studies for (a) APDC-nickel(II) and (b) AMDC-nickel(II) system with DPP-CHW.

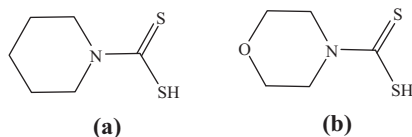


Figure 7 Two dimensional representations of (a) Piperidine and (b) Morpholine adducts with CS_2 .

nickel(II), taking into account randomization for even distribution, as illustrated in Fig. 1.

2.6. Data analysis

STATGRAPHICS *Plus* version 5.1 and Microsoft excel® 2010 were used for data evaluation and preparation of the experimental design. Peak evaluation was performed with 797 PC Software 1.3® 2008.

3. Results and discussion

3.1. Analysis of variance on analyte responses

The standardized pareto charts in Fig. 2a–b show the estimates in a decreasing order of importance. The ANOVA results reported in Table 2 describe the variability in current response

into separate pieces for each of the effects. The statistical significance of each effect shown in the pareto charts was tested by comparing the mean square deviation against an estimate of the experimental error. With regard to experiment 1 (APDC), only one effect (scan rate) had a P -value < 0.05 , and the 85.59% of the variability in analyte was explained by the model based on the R -squared value. In the case of experiment 2 (AMDC), three effects (pH, concentration of ligands, scan rate) A : pH, AA and AB had P -values of 0.0028, 0.0225 and 0.0419 respectively, which were < 0.05 . This is a clear indication that they are significantly different from zero at the 95.0% confidence level, while the R -squared statistic indicated that the model demonstrated a 90.89% of the variability in nickel(II) responses. Furthermore, a multifactor analysis of variance for the current response was performed to test significant interactions amongst the factors, using sufficient data obtained through the Box–Beckhen experimental design. With regard to experiment 1, multifactor analysis of variance showed that all the tested factors were statistically insignificant at the 90.0% confidence level, with pH having the lowest P -values close to 0.05. The highest P value was 0.546 belonging to the concentration of AMDC, while in experiment 2 it was 0.856 from the scan rate. Since the P -value in both the experiments was greater than 0.05, there was no indication of serial autocorrelation in the residuals. Further analyses of the extent of the confounding variables amongst the effects were evaluated by the correlation matrix of the three pairs. For the highest scan rate and pH, the peaks

Table 3 DFT calculations results for (a) piperidine and (b) morpholine adducts with CS_2 using three different basis sets.

	(a)b3lyp/6–31 g**	(b)b3lyp/6–31 g**	(a)b3lyp/6–311 g**	(b)b3lyp/6–311 g**
Total E (AU)	–1086.4150964	–1122.2997245	–1086.52808894	–1122.42632949
E_{HOMO} (kcal/mol)	–130.52	–134.58	–135.30	–139.44
E_{LUMO} (kcal/mol)	–16.70	–21.50	–22.82	–27.24
ΔE (kcal/mol)	–113.82	–113.08	–112.48	–112.20

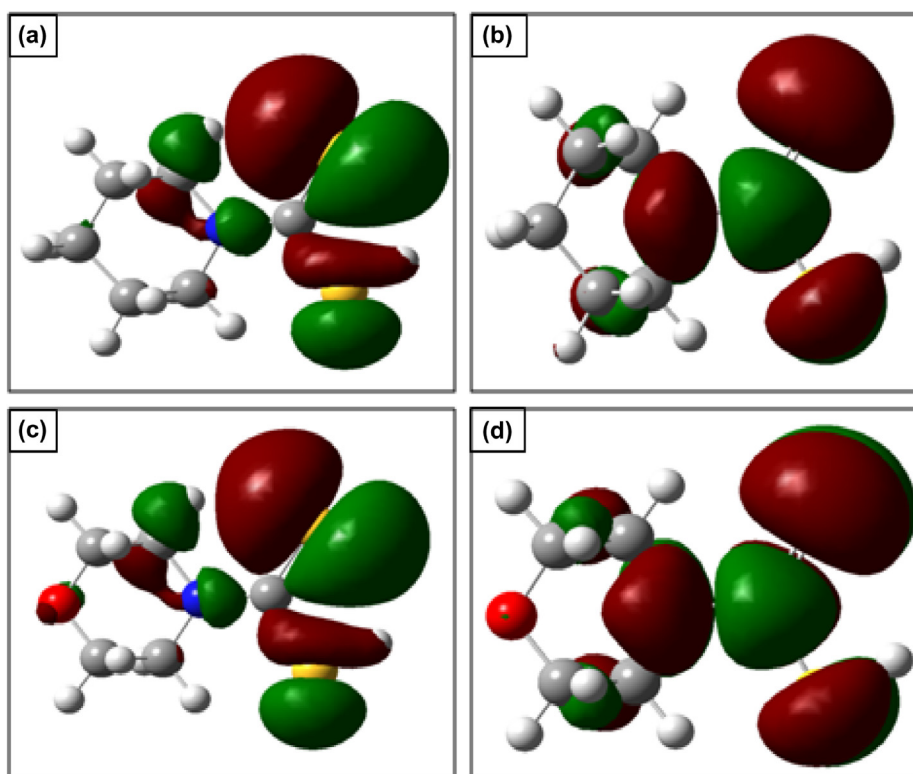


Figure 8 Electron density of (a) HOMO and (b) LUMO for piperidine and electron density of (c) HOMO and (d) LUMO for morpholine, adducts with CS_2 , computed at b3lyp/6-31 g** energy level.

Table 4 Combination of factor levels which maximizes analyte over the indicated region.

Factor	Low	High	Optimum	
			APDC	AMDC
pH	3.0	9.0	3.0	3.0
Conc of DTCs/mM	1.0	5.0	5.0	1.0
Scan rate/(mV/s)	3.0	9.0	8.2	3.1

were much broader and their potential was more positive as shown in Table 1.

3.2. Analysis of Box–Behnken design

For each factor, the zone of the experimental domain corresponding to a high value of peak heights deduced from the response surfaces was selected as the proper experimental domain. Thus the interaction plots for the nickel(II) current signals presented in Fig. 3a–b, were based on (+) and (–) values showing the maximum and minimum values of each parameter respectively (Rioa et al., 2005). These interaction plots also showed the estimated variable as a function of pairs of factors. In Fig. 3b, it can be seen that the important interaction exists between pH and concentration of AMDC (positive), which is more important than the effects of pH alone. This is highlighted in Fig. 3d, where the lowering of the pH leads to a better current response. However, when the same experiment was conducted with the APDC, a marginable in-

crease in current was observed at a lower pH, as shown in Fig. 3a. This result suggests the dependency of the mechanism of detection of the protons from the ligands, due to the zero valent metal complex at the electrode. Surface plots shown in Fig. 3c–d represent the simultaneous effect of pH, concentration of the ligand and scan rate on the current signal by nickel(II). The scan rate was kept constant at 3.0 mV/s and 8.0 mV/s for experiments 1 and 2 respectively. Very little effect of the concentration of APDC on the nickel(II) current signal was observed (Fig. 3) within the selected range, however with a decrease in pH, nickel(II) current signal improved to the highest value of approximately 2400 nA at pH 3.0 for a 1.0 ppm standard. Furthermore, the models predicted that the path of steepest descent for the analyte response was from pH 6.0 onwards. This is the path from the centre of the experimental region along which the estimated response changes rapidly for the smallest change in the experimental factors. In both the experiments, there are six points that were generated as the path of steepest descent by changing the pH in increments of 1.0 (results not shown). Beyond the main effects on current response by each factor, the experimental design further revealed that there was a significant interaction between pH and concentration, and between pH and scan rate. These interactions were more predominant in experiment 1 as can be seen in the pareto charts shown in Fig. 2. Further analysis showing the extent of the confounding variables is shown in Fig. 4a–b. In these models there are three pairs of effects shown in the interaction diagrams, and they show non-zero correlations. However, we decided to focus on the concentration of the DCs and pH, since they influenced prominently both experiments as can be seen in the pareto chart in Fig. 2. Both the contours of

Table 5 Levels of nickel(II) in red and white grape samples obtained with APDC using the DPP-CHW technique.

Sample	APDC							
	Red grapes				White grapes			
	Nickel(II) found($\mu\text{g L}^{-1}$)				Nickel(II) found($\mu\text{g L}^{-1}$)			
	Washed		Unwashed		Washed		Unwashed	
Epicarp(SD) ^a	Endocarp(SD) ^a	Epicarp(SD) ^a	Endocarp(SD) ^a	Epicarp(SD) ^a	Endocarp(SD) ^a	Epicarp(SD) ^a	Endocarp(SD) ^a	
<i>Local market</i>								
1	2.32(0.25)	2.25(0.22)	6.45(0.13)	6.90(0.19)	3.48(0.15)	3.55(0.33)	8.05(0.20)	9.20(0.48)
2	2.46(0.13)	2.10(0.35)	5.98(0.25)	6.37(0.20)	2.95(0.24)	2.39(0.10)	8.23(0.15)	9.62(0.30)
3	2.05(0.30)	2.50(0.10)	6.33(0.05)	7.41(0.18)	3.06(0.38)	3.91(0.45)	8.46(0.40)	9.85(0.22)
4	2.17(0.15)	2.36(0.15)	7.05(0.27)	7.15(0.10)	3.29(0.35)	3.46(0.24)	7.88(0.15)	9.07(0.29)
5	2.28(0.33)	2.43(0.30)	6.52(0.20)	7.00(0.45)	3.13(0.10)	2.90(0.20)	8.69(0.30)	8.92(0.46)
<i>Farm house</i>								
1	2.31(0.10)	2.90(0.25)	6.58(0.35)	7.00(0.41)	3.39(0.20)	3.50(0.10)	7.99(0.14)	9.15(0.36)
2	2.05(0.22)	2.45(0.39)	5.71(0.32)	6.55(0.28)	3.18(0.19)	2.65(0.05)	8.31(0.42)	9.64(0.30)
3	2.73(0.61)	2.84(0.20)	6.30(0.14)	7.36(0.26)	3.00(0.26)	3.86(0.17)	8.45(0.30)	9.90(0.40)
4	2.22(0.48)	2.13(0.19)	7.43(0.25)	7.05(0.44)	3.21(0.59)	3.46(0.25)	7.93(0.31)	9.10(0.10)
5	2.89(0.30)	2.20(0.28)	6.44(0.26)	7.10(0.13)	3.10(0.38)	2.94(0.29)	8.72(0.20)	8.95(0.35)

^a Standard deviation (SD) average reported for three individual replicates; Epicarp: Grape peel, Endocarp: Grape pulp + seeds.

Table 6 Levels of nickel(II) in red and white grape samples obtained with AMDC using the DPP-CHW technique.

Sample	AMDC							
	Red grapes				White grapes			
	Nickel(II) found($\mu\text{g L}^{-1}$)				Nickel(II) found($\mu\text{g L}^{-1}$)			
	Washed		Unwashed		Washed		Unwashed	
Epicarp(SD) ^a	Endocarp(SD) ^a	Epicarp(SD) ^a	Endocarp(SD) ^a	Epicarp(SD) ^a	Endocarp(SD) ^a	Epicarp(SD) ^a	Endocarp(SD) ^a	
<i>Local market</i>								
1	2.32(0.25)	2.25(0.22)	6.45(0.13)	6.90(0.19)	3.48(0.15)	3.55(0.33)	8.05(0.20)	9.20(0.48)
2	2.46(0.13)	2.10(0.35)	5.98(0.25)	6.37(0.20)	2.95(0.24)	2.39(0.10)	8.23(0.15)	9.62(0.30)
3	2.05(0.30)	2.50(0.10)	6.33(0.05)	7.41(0.18)	3.06(0.38)	3.91(0.45)	8.46(0.40)	9.85(0.22)
4	2.17(0.15)	2.36(0.15)	7.05(0.27)	7.15(0.10)	3.29(0.35)	3.46(0.24)	7.88(0.15)	9.07(0.29)
5	2.28(0.33)	2.43(0.30)	6.52(0.20)	7.00(0.45)	3.13(0.10)	2.90(0.20)	8.69(0.30)	8.92(0.46)
<i>Farm house</i>								
1	2.20(0.15)	2.63(0.10)	6.39(0.25)	7.12(0.48)	3.17(0.33)	3.36(0.21)	7.77(0.40)	8.90(0.38)
2	2.00(0.35)	2.26(0.30)	5.50(0.20)	6.33(0.06)	3.10(0.10)	2.44(0.25)	8.29(0.62)	9.52(0.39)
3	2.81(0.68)	2.63(0.42)	6.29(0.17)	7.25(0.10)	2.92(0.29)	3.60(0.43)	8.40(0.12)	9.86(0.30)
4	2.11(0.25)	1.99(0.32)	7.30(0.13)	7.14(0.28)	3.18(0.55)	3.31(0.15)	7.82(0.18)	9.02(0.34)
5	2.72(0.14)	2.00(0.20)	6.37(0.04)	7.06(0.22)	3.15(0.61)	3.05(0.23)	8.65(0.13)	8.82(0.48)

^a Standard deviation(SD) average reported for three individual replicates; Epicarp: Grape peel, Endocarp: Grape pulp + seeds.

the surface responses showed a diagonal matrix with 1's on the diagonal and 0's off the diagonal for pH around 7.0. The distance between the diagonal lines tends to increase as the pH increases; this justified the low optimum values of the pH obtained.

3.3. Electrochemical studies

Scheme 1 shows the structures of the APDC/AMDC considered in this study. They form co-ordination with the sulphur atoms of DCs, being noteworthy for their remarkable versatility as a strong chelating agent. In the DPP-CHW methodology, nickel(II) forms a complex with APDC/AMDC, which subsequently absorbs onto the DME working electrode during

the deposition step. During the polarographic scan, nickel(II)-Dithiocarbamate $[\text{Ni}^{+2} - \text{DC}]_{\text{ads}}$ complex is reduced to $[\text{Ni}^0 - \text{DC}]_{\text{ads}}$ which undergoes protonation by accepting proton from the solution $[\text{Ni}^0 - \text{DCH}^+]_{\text{ads}}$ in the adsorbed state, followed by the reduction to liberate hydrogen in the presence of mercury electrode, as shown in Eqs. 1–3 below:



M = Metal ion, RS = Dithiocarbamate

Table 7 Analytical data for the nickel(II) present in whole grape sample (red and white) with APDC/AMDC using the DPP-CHW technique.

Sample	Whole grape			
	Nickel(II) found ($\mu\text{g L}^{-1}$)			
	Red grape		White grape	
	Local market(SD) ^a	Farm(SD) ^a	Local market(SD) ^a	Farm(SD) ^a
<i>APDC</i>				
1	8.23(0.260)	9.28(0.16)	8.62(0.15)	9.73(0.36)
2	8.78(0.18)	9.93(0.25)	8.90(0.08)	9.80(0.14)
3	8.12(0.30)	9.59(0.41)	8.98(0.25)	9.98(0.30)
4	8.57(0.45)	9.70(0.62)	8.51(0.42)	9.35(0.15)
5	8.36(0.22)	8.99(0.10)	8.11(0.31)	9.52(0.26)
<i>AMDC</i>				
1	8.00(0.42)	9.12(0.15)	8.34(0.30)	9.65(0.16)
2	8.53(0.18)	9.60(0.25)	8.76(0.45)	9.72(0.25)
3	7.94(0.21)	9.47(0.64)	8.70(0.18)	9.69(0.31)
4	8.40(0.14)	9.55(0.38)	8.45(0.10)	9.40(0.46)
5	8.05(0.48)	8.76(0.20)	8.10(0.25)	9.38(0.54)

^a Standard deviation(SD) average reported for three individual replicates.

Cyclic voltammetry (CV) carried out at pH 3.0 was utilized to confirm the possible complexation reaction between nickel and APDC/AMDC as illustrated in Fig. 5a–d. The voltammetric behaviour in the absence of nickel(II) is shown in Fig. 5a–b for APDC and AMDC respectively. In the case of APDC, two reversible peaks are predominant, where during a cathodic scan one corresponds to a reduction at $E_p = -0.43$ V and a sharper and more pronounced oxidation peak appeared during the anodic scan at -0.5 V (vs. Ag/AgCl). Similar shaped voltammograms were obtained for AMDC, except that both peaks shifted to more negative peak potentials, as illustrated in Fig. 5b. It is believed that this behaviour was mainly due to the presence of 'O' in the morpholine ring (Kanchi et al., 2013; Morsi et al., 2011). However evidence for the nickel-complex formation of APDC and AMDC is depicted in Fig. 5c–d respectively. Interestingly, nickel(II)-AMDC complex yielded a more pronounced reduction peak and oxidation peaks, in contrast to nickel(II)-APDC complex.

Therefore, oxidation of DCs at the HMDE is represented as



RSH = Dithiocarbamate

in agreement with the earlier reports in the literature (Stricks and Chakravarthi, 1962). The typical polarograms were recorded at $E_{1/2} = -1.22$ V for both APDC/AMDC-nickel(II) complex systems after optimization studies using DPP-CHW as shown in Fig. 6a–b.

3.4. Computational studies

The electron-donating tendencies of piperidine (Fig. 7a) and morpholine (Fig. 7b) adducts with carbon disulphide (CS_2) were monitored by performing their density functional theory (DFT) calculations using the computer Gaussian program (Frisch et al., 2003). The initial structures of both adducts were geometrically optimized at the B3LYP (DFT) level using 6–31 g^{**} and 6–311 g^{**} basis sets. The global minimum for each

optimized geometry was further confirmed by a frequency calculation. The energy differences (ΔE) between the highest occupied molecular orbital (HOMO) and the lowest unoccupied molecular orbital (LUMO) are considered to be an important parameter which defines the chemical activity of any compound, with the smaller value indicating a stronger tendency to donate electrons. Accordingly, the HOMO and LUMO of both piperidine and morpholine adducts were generated, and the energy data are summarized in Table 3. The HOMO–LUMO of structures, obtained using 6–31 g^{**} basis sets, are depicted in Fig. 8a–d. Generally, the distribution of electrons in HOMO and LUMO of both complexes was almost similar (Fig. 8a–d). As expected, the electron density of both piperidine (Fig. 8a) and morpholine (Fig. 8c) adducts was mostly localized on the sulphur atoms, suggesting a stronger propensity of these atoms to participate in the complexation with the electron deficient species including metals. However in case of piperidine, the comparatively lower energy gaps (ΔE) between HOMO and LUMO shown in Table 3, suggest a better tendency to act as an electron donor and support the DPP studies, where the intensity of current was observed to be higher in case of piperidine-nickel(II) complex, than with the morpholine-nickel(II) complex. It is believed that the negative inductive effect (-I effect) of the oxygen atom in the morpholine adduct, reduces the electron density on its nitrogen atom through the intervening electrons of the bonds, and probably accounts for the higher ΔE values shown in Table 3. Based on these results, it is believed that the energy barrier between HOMO and LUMO of ligands could be a very useful parameter to predict their binding affinities in metal complexation, and could therefore play a pivotal role in identifying the more efficient and sensitive ligands in the field of electroanalytical chemistry.

3.5. Analytical applications

The proposed DPP-CHW technique was applied for the analysis of nickel(II) in different grape samples, using the optimum parameters (shown in Table 4) obtained through the Box Behn-

Table 8 Determination of nickel(II) in spiked red and white grape samples.

Sample	Nickel(II) spiked($\mu\text{g L}^{-1}$)	Red grape			White grape				
		Local market			Farm				
		Found(SD) ^a	% Recovery(RSD) ^b	Found(SD) ^a	Found(SD) ^a	% Recovery(RSD) ^b	Found(SD) ^a	% Recovery(RSD) ^b	
<i>APDC</i>									
Epicarp	10	12.19(0.18)	99.00(2.38)	12.72(0.25)	99.00(2.50)	13.92(0.06)	100.00(3.46)	14.36(0.36)	99.80(3.36)
Endocarp	15	17.99(0.26)	99.86(2.94)	18.56(0.20)	99.86(3.15)	19.55(0.19)	99.80(2.98)	20.40(0.28)	99.93(3.72)
Whole Grape	20	22.44(0.62)	99.55(3.18)	26.88(0.45)	99.99(3.46)	27.58(0.40)	99.80(3.17)	29.88(0.55)	99.85(2.90)
<i>AMDC</i>									
Epicarp	10	11.89(0.26)	98.90(2.46)	12.69(0.15)	99.00(3.16)	12.55(0.09)	99.00(2.61)	13.63(0.42)	99.65(3.40)
Endocarp	15	17.46(0.39)	99.66(2.18)	18.38(0.40)	99.53(1.99)	19.26(0.25)	99.73(3.20)	19.71(0.20)	99.83(2.92)
Whole Grape	20	22.10(0.05)	99.35(3.42)	26.07(0.33)	99.70(3.40)	27.39(0.37)	99.45(2.19)	28.95(0.36)	99.50(2.30)

^a Standard deviation(SD) average reported for three individual replicates.^b Relative standard deviation for six individual replicates, Epicarp: Grape peel, Endocarp: Grape pulp + seeds, Whole grape: Epicarp + Endocarp + seeds.

ken experimental design. Different grape samples were collected from local markets and directly from the farm houses. Samples were treated as described in the experimental section before the quantification of nickel(II). The obtained data are summarized in Tables 5–8.

In this study, 92 different forms of grape (red and white) samples were analysed for the determination of nickel(II). Significant differences of nickel(II) concentrations were observed between the epicarp, endocarp and the whole grape samples collected from local markets and farm houses. On the whole, no significant differences between the samples (epicarp, endocarp and whole grape) were observed. Table 8, clearly shows that the recoveries of nickel(II) were higher with APDC than with AMDC, which was indicative of the sensitivity of APDC. This study was carried out with three different concentrations ranging from 10.0 to 20.0 $\mu\text{g L}^{-1}$. Overall, for both ligands (APDC/AMDC), recoveries obtained were always higher than 97.0% as shown in Table 8.

3.6. Comparison of the DPP-CHW method with reported methods

Table 9 shows the comparison of multivariate optimization voltammetric determination of nickel(II) in real samples with other methods reported in the literature. The LOQ's for APDC & AMDC are 2.7×10^{-6} and 1.8×10^{-6} M respectively for the determination of nickel(II) in different grape samples, that are better than those reported in the literature (Dadfarnia et al., 2010). Additionally, the APDC/AMDC could be considered as more promising and also cost effective chelating agents for the analysis of nickel(II), in contrast to those reported in the literature [C4MIM][PF6] (Dadfarnia et al., 2010) MSOPD (Khorrami et al., 2004) and Py-MCM-48 (Sadeghi et al., 2011). Although previously reported chelating agents such as EDTA (Baytak and Turker, 2006), MSOPD (Khorrami et al., 2004), PAN (Bidabadi et al., 2009) and Py-MCM-48 (Sadeghi et al., 2011) are sensitive than the current APDC/AMDC, the methods employed required more solvent (SPE, LLE) with an elaborate sampling procedure utilizing sophisticated instrumentation such as FI-FAAS, ETAAS and GFAAS. Accordingly, the present method for the determination of nickel(II) in real samples therefore is facile, sensitive, economical and environmentally friendly.

3.7. Effect of foreign ions

In the present study, various heavy metal ions commonly associated with nickel(II) such as aluminium(III), chromium(VI), zinc(II), molybdenum(VI), selenium(IV), tellurium(IV), cerium(IV) and tin(II) have been evaluated for their impact in the DPP-CHW of dithiocarbamate-nickel(II) system. In particular, the concentration of nickel(II) was maintained at 4.0 ppm with a 100 fold excess of foreign ions added. Among the metal ions studied, iron(II) and copper(II) formed precipitates with DCs in the conditions where nickel(II)-dithiocarbamate complex yielded a CHW. Aluminium(III) did not interfere whereas chromium(VI) gave a CHW with peak potentials at -1.56 V and -1.65 V vs Ag/AgCl, suggesting that a simultaneous determination of nickel(II) & chromium(VI) was feasible without any separation or adding masking agents. Zinc(II) interfered in the determination of nickel(II), but were

Table 9 Comparison of analytical parameters with the reported methods.

Method	Instrument	Ligands	Matrix	LOD	LOQ	Citations
LLE	FI-FAAS	[C4MIM][PF6]	Rice flour, Black tea, Tap water, Well water, River water, Sea water	12.5 g L ⁻¹	41.0 g L ⁻¹	Shayesteh et al. (2010)
SPE	FAAS	EDTA	Tea leaves, Parsley green onion, Waste water, Sea water	1.42 ng mL ⁻¹	–	Sitki and Rehber (2006)
SPE	FAAS	MSOPD	Tap water, River water, Sea water, Synthetic samples	30 ng L ⁻¹	–	Afshin et al. (2004)
SFODME	GFAAS	PAN	Tap water, River water, Well Water Sea water	0.3 ng L ⁻¹	1.0 ng L ⁻¹	Mahboubeh et al. (2009)
SPE	ETAAS	Py-MCM-48	Digested vegetables	0.14 ng mL ⁻¹	–	Sadeghi et al. (2011)
DPP-CHW	DPP	APDC/AMDC	Grape (red & white) samples	2.7 × 10 ⁻⁶ /1.8 × 10 ⁻⁶ M	3.2 × 10 ⁻⁶ M	This study

LLE: Liquid-liquid extraction, SPE: Solid phase extraction, SFODME: Solidified floating organic drop microextraction, DPP-CHW: Differential pulse polarographic-catalytic hydrogen wave, FI-FAAS: Flow injection-flame atomic absorption spectrometry, FAAS: Flame atomic absorption spectrometry, GFAAS: Graphite furnace atomic absorption spectrometry, ETAAS: Electrothermal atomic adsorption spectroscopy, DPP: Differential pulse polarography, [C4MIM][PF6]: 1-butyl-3-methylimidazolium hexafluorophosphate, EDTA: Ethylenediaminetetraacetic acid, MSOPD: *N,N*-bis (3-methylsallylidene) ortho phenylene diamine, DMG: Dimethylglyoxime, PAN: 1-(2-Pyridylazo)-2-naphthol, Py-MCM-48: pyridine-functionalized MCM-48 mesoporous silica, APDC/AMDC: Ammonium piperidine dithiocarbamate/Ammonium morpholine dithiocarbamate.

masked by adding 5.0 mL of 2% sodium tartrate solution. Molybdenum(VI) severely interfered by increasing the peak height of nickel(II) and shifting the peak potentials towards a more negative value. The selenium(IV), tellurium(IV), cerium(IV) and tin(II) also did not interfere with the nickel(II)-dithiocarbamate system. Anions such as fluoride, bromide, iodide, tartrate, sulphate, thiosulphate, phosphate, carbonate, oxalate, nitrite and nitrate did not interfere with the CHW of dithiocarbamates-nickel(II) system. Perchlorate and thiocyanate interfered with the wave by reducing the wave height by approximately 40.0% and EDTA interferes severely by completely suppressing the nickel(II) catalytic hydrogen wave.

4. Conclusions

The DPP-CHW technique proved to be a facile, rapid, sensitive and robust approach for the determination of nickel(II) in different grape samples. The limit of detection for the determination of nickel(II) was 1.8×10^{-6} and 2.7×10^{-6} M for APDC and AMDC respectively. They both act as unique ligands due to their free thiols and also the ease (one step) of synthesis. In experiment 2, AMDC showed a greater flexibility as three effects had a $p < 0.05$, in contrast to experiment 1 performed with APDC, which had only a single effect. From the optimization point of view, our results suggest that it is easier to work with APDC, since one needs to be more conscious of only the pH being the most effective parameter. In this regard, the experimental design was therefore convenient to evaluate the statistical significance of the variation in current responses due to factor variations and optimization of the related parameters as confirmed by the interaction plots, contours and response surface plots. Finally, the electron donating tendencies of APDC and AMDC assessed in terms of their HOMO-LUMO energy gaps calculated at DFT level strongly supported our DPP experimental findings, and could therefore be used as preliminary predictions for oxidation/reduction capabilities of the new ligands.

Acknowledgements

The authors gratefully acknowledge the financial support received from the Durban University of Technology (DUT) and National Research Foundation (NRF) of South Africa. The authors would like to express their acknowledgement to the Centre for High Performance Computing, an initiative supported by the Department of Science and Technology of South Africa.

References

- Amin, Alaa S., Amirah, S., AL-Attas, 2012. Study of the solid phase extraction and spectrophotometric determination of nickel using 5-(4'-chlorophenylazo)-6-hydroxypyrimidine-2*4-dione in environmental samples. *J. Saud. Chem. Soc.* 6 (4), 451-459.
- Armstrong, R.D., Todd, M., Atkinson, J.W., Scott, K., 1997. Electro-separation of cobalt and nickel from a simulated waste water. *J. Appl. Electrochem.* 27, 965-970.
- Baytak, Sitki., Rehber Turker, A., 2006. Determination of lead and nickel in environmental samples by flame atomic absorption

- spectrometry after column solid-phase extraction on Ambersorb-572 with EDTA. *J. Hazard. Mater.* 129 (1–3), 130–136.
- Beiraghi, Assadollah, Babae, Saeed, Roshdi, Mina, 2012. Simultaneous preconcentration of cadmium, cobalt and nickel in water samples by cationic micellar precipitation and their determination by inductively coupled plasma-optical emission spectrometry. *Microchem. J.* 100, 66–71.
- Bencko, V., 1983. Nickel: a review of its occupational and environmental toxicology. *J. Hyg. Epidem. Microbiol. Immun.* 27, 237–247.
- Bidabadi, Mahboubeh Shirani, Dadfarnia, Shayessteh, Shabani, Ali Mohammad Haji, 2009. Solidified floating organic drop microextraction (SFODME) for simultaneous separation/preconcentration and determination of cobalt and nickel by graphite furnace atomic absorption spectrometry (GFAAS). *J. Hazard. Mater.* 166 (1), 291–296.
- Box, G., Meyer, D., 1986. Dispersion effects from factorial designs. *Technometrics* 28, 11–26.
- Carlson, R., 1992. Design and optimization in organic synthesis. Elsevier, Amsterdam.
- Clarkso, N.T.W., 1988. Biological Monitoring of Toxic Metals. Plenum Press, New York, pp. 265–273.
- Colombo, C., Van der Berg, C.M.G., 1998. Determination of trace metals (Cu, Pb, Zn and Ni) in soil extracts by flow analysis with voltammetry detection. *Int. J. Environ. Anal. Chem.* 71, 1–17.
- Cott Fordsmand, J.J., 1997. Toxicity of nickel to soil organisms in Denmark. *Rev. Environ. Contam. Toxicol.* 148, 1–7.
- Dadfarnia, Shayessteh, Shabani, Ali Mohammad Haji, Bidabadi, Mahboubeh Shirani, Jafari, Abbas Ali, 2010. A novel ionic liquid/micro-volume back extraction procedure combined with flame atomic absorption spectrometry for determination of nickel in samples of nutritional interest. *J. Hazard. Mater.* 173 (1–3), 534–538.
- Deng, Qingwen, Chen, Meihui, Kong, Lamei, Zhao, Xia, Guo, Jie, Xiaodong, Wen, 2013. Novel coupling of surfactant assisted emulsification dispersive liquid-liquid microextraction with spectrophotometric determination of ultratrace nickel. *Spectrochim. Acta Part A: Mol. Biomol. Spectrosc.* 104, 64–69.
- Dobrowolski, Ryszard, Otto, Magdalena, 2012. Determination of nickel and cobalt in reference plant materials by carbon slurry sampling GFAAS technique after their simultaneous preconcentration onto modified activated carbon. *J. Food Comp. Anal.* 26 (1–2), 58–65.
- Economou, A., Fielden, P.R., 1998. Selective determination of Ni(II) and Co(II) by flow injection analysis and adsorptive cathodic stripping voltammetry on a wall jet mercury film electrode. *Talanta* 46, 1137–1146.
- Fakhari, Ali Reza, Khorrami, Afshin Rajabi, Naeimi, Hossein, 2005. Synthesis and analytical application of novel tetradentate N_2O_2 schiff's base as a chromogenic reagent for determination of nickel in some natural food samples. *Talanta* 66 (4), 813–817.
- Flora, C.J., Nieboer, E., 1980. Determination of nickel by differential pulse polarography at dropping mercury electrode. *Anal. Chem.* 52, 1013–1020.
- Frisch, M.J., Trucks, G.W., Schlegel, H.B., Scuseria, G.E., Robb, M.A., Cheeseman, J.R., Montgomery, J.A., Jr, Vreven, T., Kudin, K.N., Burant, J.C., Millam, J.M., Iyengar, S.S., Tomasi, J., Barone, V., Mennucci, B., Cossi, M., Scalmani, G., Rega, N., Petersson, G.A., Nakatsuji, H., Hada, M., Ehara, M., Toyota, K., Fukuda, R., Hasegawa, J., Ishida, M., Nakajima, T., Honda, Y., Kitao, O., Nakai, H., Klene, M., Li, X., Knox, J.E., Hratchian, J.P., Cross, J.B., Adamo, C., Jaramillo, J., Gomperts, R., Stratmann, R.E., Yazyev, O., Austin, A.J., Cammi, R., Pomelli, C., Ochterski, J.W., Ayala, P.Y., Morokuma, K., Voth, G.A., Salvador, P., Dannenberg, J.J., Zakrzewski, V.G., Dapprich, S., Daniels, A.D., Strain, M.C., Farkas, O., Malick, D.K., Rabuck, A.D., Raghavachari, K., Foresman, J.B., Ortiz, J.V., Cui, Q., Baboul, A.G., Clifford, S., Cioslowski, J., Stefanov, B.B., Liu, G., Liashenko, A., Piskorz, P., Komaromi, I., Martin, R.L., Fox, D.J., Keith, T., Al-Laham, M.A., Peng, C.Y., Nanayakkara, A., Challacombe, M., Gill, P.M.W., Johnson, B., Chen, W., Wong, M.W., Gonzalez, C., Pople, J.A., 2003. Gaussian 03, Revision, A1, Gaussian, Inc., Wallingford, CT, USA.
- Furlanetto, S., Maestrelli, F., Orlandini, S., Pinzauti, S., Mura, P., 2003. Optimization of dissolution test precision for a ketoprofen extended-release product. *J. Arm. Biomed. Anal.* 32, 159–165.
- Ghaedi, M., Ahmadi, F., Soylak, M., 2007. Preconcentration and separation of nickel, copper and cobalt using solid phase extraction and their determination in some real samples. *J. Hazard. Mater.* 147 (1–2), 226–231.
- González, P., Cortínez, V.A., Fontá, C.A., 2002. Voltammetric method for direct determination of nickel in natural waters in the presence of surfactants. *Talanta* 58 (4), 679–686.
- Grandjean, P., 1984. Human exposure to nickel. *IARC Sci. Publ.* 53, 469–473.
- Green, J.M., 1996. A practical guide to analytical method validation. *Anal. Chem.* 68, 305–309.
- Hemasundaram, H., 2006. A study on the status of trace metals in environmental and biological samples, Ph.D Thesis, S.V. University, pp. 90.
- Hussain Reddy, K., Prasad, N.B.L., Sreenivasulu Reddy, T., 2003. Analytical properties of 1-phenyl-1,2-propanedione-2-oxime thiosemicarbazone: simultaneous spectrophotometric determination of copper(II) and nickel(II) in edible oils and seeds. *Talanta* 59 (3), 425–433.
- Kanchi, S., Singh, P., Sabela, M.I., Bisetty, K., Venkatasubba Naidu, N., 2013. Polarographic catalytic hydrogen wave technique for the determination of copper(II) in leafy vegetables and biological samples. *Int. J. Electrochem. Sci.* 8, 4260–4282.
- Kasprzak, K.S., Sunderman, F.W., Salnikow, K., 2003. Nickel carcinogenesis. *Mutat. Res.* 533 (1–2), 67–72.
- Khorrami, Afshin Rajabi, Naeimi, Hossein, Fakhari, Ali Reza, 2004. Determination of nickel in natural waters by FAAS after sorption on octadecyl silica membrane disks modified with a recently synthesized schiff's base. *Talanta* 64 (1), 13–17.
- Korolczuk, Mieczyslaw, 2000. Voltammetric method for direct determination of nickel in natural waters in the presence of surfactants. *Talanta* 53 (3), 679–686.
- Lewis, G.A., Mathieu, D., Phan Tan Luu, R., 1999. Pharmaceutical Experimental Design. Dekker, New York.
- Loka, Subramanyam Sarma, Jyothi, Rajesh Kumar, Koduru, Janardhan Reddy, Thenepalli, Thriveni, Ammireddy, Varada Reddy, 2008. Development of highly sensitive extractive spectrophotometric determination of nickel(II) in medicinal leaves, soil, industrial effluents and standard alloy samples using pyridoxal-4-phenyl-3-thiosemicarbazone. *J. Trace Elem. Med. Bio.* 22 (4), 285–295.
- Mathieu, D., Phan-Tan-Luu, R., Sergent, M., 1998. Methodes modernes d'elaboration de matrices d'experiences optimales et qualite. LPRAI, Marseille.
- Merck and Co. Inc., 1983. The Merck Index. 10th ed., Rahway, New York.
- Montgomery, D.C., 1997. Design and Analysis of Experiments. Wiley New York.
- Morsi, M.A., Hilmey, A.M.A., Etman, H.A., Ouf, A.M.A., 2011. Determination of lead by square wave adsorptive stripping voltammetry using ammonium pyrrolidine dithiocarbamates. *J. Am. Sci.* 7 (6), 1173–1179.
- Pieniaszek, H.J., 1999. Short course on bioanalytical method development, validation and transfer. 10th International Symposium on Pharmaceutical and Biomedical Analysis, Washington, D.C., USA.
- Polaskova, P., Bocaz, G., Li, H., Havel, J., 2002. Evaluation of calibration data in capillary electrophoresis using artificial neural networks to increase precision of analysis. *J. Chromatogr. A.* 979, 59–67.

- Ramachandraiah, C., Rajesh Kumar, J., Janardhan Reddy, K., Lakshmi Narayana, S., Varada Reddy, A., 2008. Development of a highly sensitive extractive spectrophotometric method for the determination of nickel(II) from environmental matrices using N-ethyl-3-carbazolecarboxaldehyde-3-thiosemicarbazone. *J. Environ. Manag.* 88 (4), 729–736.
- Rioa, Sebastien, Faur-Brasqueta, Catherine, Le Coqa, Laurence, Courcouxb, Philippe, Le Cloireca, Pierre, 2005. Experimental design methodology for the preparation of carbonaceous sorbents from sewage sludge by chemical activation-application to air and water treatment. *Chemosphere* 58 (4), 423–437.
- Sadeghi, O., Tavassoli, N., Amini, M.M., Ebrahimzadeh, H., Daei, N., 2011. Pyridine-functionalized mesoporous silica as an adsorbent materials for the determination of nickel and lead in vegetables grown in close proximity by electrothermal atomic adsorption spectroscopy. *Food Chem.* 127 (1), 364–368.
- Şahin, Cigdem Arpa, Efecinar, Melis, Satiroglu, Nuray, 2010. Combination of cloud point extraction and flame atomic absorption spectrometry for preconcentration and determination of nickel and manganese ions in water and food samples. *J. Hazard. Mater.* 176 (1–3), 672.
- Sancho, Daniel, Debán, Luis, Campos, Isabel, Pardo, Rafael, Vega, Marisol, 2000. Determination of nickel and cobalt in refined bet sugar by adsorptive cathodic stripping voltammetry without sample pretreatment. *Food Chem.* 71 (1), 139–145.
- Saraswathi, K., Naidu, N.V.S., Suresh, G., Dhanalakshmi, K., 2006. Polarographic study of Ni(II)-xanthate systems at mercury electrode. *Bull. Elec. Chem.* 22 (1), 1–5.
- Silva, Edson Luiz, Roldan, Paulo dos Santos, Gine, Maria Fernanda, 2009. Simultaneous preconcentration of copper, zinc, cadmium and nickel in water samples by cloud point extraction using 4-(2-pyridylazo)-resorcinol and their determination by inductively coupled plasma optical emission spectrometry. *J. Hazard. Mater.* 171 (1-3), 1133–1138.
- Spectrum, Chemical Fact Sheet. Nickel., 1998. Web site: <<http://www.speclab.com/elements/nickel.htm>> (accessed 03.03.2005).
- Stricks, W., Chakravarthi, S.K., 1962. Polarography of diethyldithiocarbamate, a titrant with a rotated dropping mercury indicator electrode. *Anal. Chem.* 34, 508–513.
- Sun, Zhimei, Liang, Pei, Ding, Qiong, Cao, Jing, 2006. Determination of trace nickel in water samples by cloud point extraction preconcentration coupled with graphite furnace atomic absorption spectrometry. *J. Hazard. Mater.* 137 (2), 943–946.
- Swartz, M.E., Krull, I., 1997. *Analytical Method Development and Validation*. Dekker, New York.
- Thomposon, M., Ellison, S., Wood, R., 2002. Harmonized guidelines for single-laboratory validation of methods of analysis (IUPAC Technical Report). *Pure Appl. Chem.* 74, 835–855.
- Von Burg, R., 1997. Toxicology update. *J. Appl. Toxicol.* 17, 425–431.
- Wang, J., Wang, J., Adeniyi, W.K., Kounaves, S.P., 2000. Adsorptive stripping analysis of trace nickel at Iridium based ultramicro electrode arrays. *Electroanalysis* 12 (1), 44–47.
- WHO, 1991. *Environmental health criteria 108: Nickel*, WHO, Geneva.
- Zeng, Chujie, Jia, Yunzhen, Lee, Yong -Ill, Hou, Xiandeng, Li, Wu, 2012. Ultrasensitive determination of cobalt and nickel by atomic fluorescence spectrometry using APDC enhanced chemical vapor generation. *Microchem. J.* 104, 33–37.